

AperTO - Archivio Istituzionale Open Access dell'Università di Torino

**On the kinetic and thermodynamic fragility of the Pt<sub>60</sub>Cu<sub>16</sub>Co<sub>2</sub>P<sub>22</sub> and Pt<sub>57.3</sub>Cu<sub>14.6</sub>Ni<sub>5.3</sub>P<sub>22.8</sub> bulk metallic glasses**

**This is the author's manuscript**

*Original Citation:*

*Availability:*

This version is available <http://hdl.handle.net/2318/153003> since

*Published version:*

DOI:10.1016/j.jallcom.2013.12.006

*Terms of use:*

Open Access

Anyone can freely access the full text of works made available as "Open Access". Works made available under a Creative Commons license can be used according to the terms and conditions of said license. Use of all other works requires consent of the right holder (author or publisher) if not exempted from copyright protection by the applicable law.

(Article begins on next page)



## UNIVERSITÀ DEGLI STUDI DI TORINO

This Accepted Author Manuscript (AAM) is copyrighted and published by Elsevier. It is posted here by agreement between Elsevier and the University of Turin. Changes resulting from the publishing process - such as editing, corrections, structural formatting, and other quality control mechanisms - may not be reflected in this version of the text. The definitive version of the text was subsequently published in [*Journal of Alloys and Compounds*, volume 651, Supplement 1, December 2014, and [doi:10.1016/j.jallcom.2013.12.006](https://doi.org/10.1016/j.jallcom.2013.12.006)].

You may download, copy and otherwise use the AAM for non-commercial purposes provided that your license is limited by the following restrictions:

- (1) You may use this AAM for non-commercial purposes only under the terms of the CC-BY-NC-ND license.
- (2) The integrity of the work and identification of the author, copyright owner, and publisher must be preserved in any copy.
- (3) You must attribute this AAM in the following format: Creative Commons BY-NC-ND license (<http://creativecommons.org/licenses/by-nc-nd/4.0/deed.en>), [[doi:10.1016/j.jallcom.2013.12.006](https://doi.org/10.1016/j.jallcom.2013.12.006) to the published journal article on Elsevier's ScienceDirect® platform]

**On the kinetic and thermodynamic fragility of the  $\text{Pt}_{60}\text{Cu}_{16}\text{Co}_2\text{P}_{22}$  and  $\text{Pt}_{57.3}\text{Cu}_{14.6}\text{Ni}_{5.3}\text{P}_{22.8}$  bulk metallic glasses**

Isabella Gallino,<sup>a</sup> Oliver Gross<sup>a</sup>, Giulia dalla Fontana<sup>b</sup>, Zach Evenson<sup>a</sup>, and Ralf Busch<sup>a</sup>

<sup>a</sup>Saarland University, Department of Materials Science and Engineering, Campus C6.3, 66123 Saarbruecken, Germany

<sup>b</sup>Department of Chemistry IFM and NIS, University of Torino, V. Giuria 7, 10125 Torino, Italy

**ABSTRACT**

The investigations in this study focus on bulk metallic glass (BMG) alloy families based on noble metals like Pt, which are more kinetically fragile than Zr-based BMG systems. Thermophysical properties have been investigated by calorimetry and thermal mechanical analyses for the determination of the specific heat capacity and viscosity, respectively. For the  $\text{Pt}_{60}\text{Cu}_{16}\text{Co}_2\text{P}_{22}$ , and  $\text{Pt}_{57.3}\text{Cu}_{14.6}\text{Ni}_{5.3}\text{P}_{22.8}$  BMG compositions consistent Vogel-Fulcher-Tammann (VFT) fits of the viscosity measurements are established, and the temperature dependence of the configurational entropy is calculated from thermodynamic data. Fits to the Adam-Gibbs equation are performed using this configurational entropy change. Their fragile nature is compared to that of Zr-based alloys in terms of structural considerations.

A. metallic glasses

C. thermodynamic properties

C. kinetics

D. calorimetry

D. thermal mechanical analysis

## 1. INTRODUCTION

The slow kinetics in bulk metallic glass (BMG) forming liquids is the main contributing factor to their high glass forming ability (GFA). Recent studies of the melt viscosity of multi-component, Zr-based BMG alloys have produced a picture of a very viscous liquid, in which the sluggish kinetics impedes the nucleation and growth of crystals [1-2]. The high viscosity originates from the large size mismatches of the liquid's many atomic species, leading to less free-volume available for viscous flow. In fact, it has been shown that the GFA of Zr-based alloys increases with an increasing number of components [3]. The underlying reason for this behavior is most likely that, with increasing number of differently sized atomic species, it becomes possible to produce higher and higher density liquids. It also makes the liquid more viscous and thus stronger in the framework of the fragility concept.

Important questions now arise as to whether slow kinetics is found in BMG formers in general, and how it depends on, for example, the alloy composition, the alloy complexity and the group of alloys. The Mg-Cu-Y BMG alloy, for example, behaves stronger than the Zr- and Ti-based alloys, which themselves behave stronger than the noble metal-based alloys [4-5]. The investigations in this study focus on the BMG alloy family based on Pt, which are more kinetically fragile than Zr-based BMG systems. Thermodynamically, once crystallized they have an entropy of fusion double that of the corresponding Pd-based alloys. The purpose of this work is therefore to determine consistent thermophysical properties related to the thermodynamics and kinetics for two different compositions,  $\text{Pt}_{60}\text{Cu}_{16}\text{Co}_2\text{P}_{22}$  and  $\text{Pt}_{57.3}\text{Cu}_{14.6}\text{Ni}_{5.3}\text{P}_{22.8}$ . Their kinetic fragilities and thermodynamic properties are discussed in terms of structural considerations.

## 2. EXPERIMENTAL AND FITTING PROCEDURES

BMG specimens of 3 mm thickness were produced using an Indutherm MC14 tilt-casting device by melting the master alloys in a boron nitride crucible, and cast in a water-cooled Cu-mold with plate geometry ( $3 \times 13 \times 34$  mm). The master alloys with composition  $\text{Pt}_{60}\text{Cu}_{16}\text{Co}_2\text{P}_{22}$  and  $\text{Pt}_{57.3}\text{Cu}_{14.6}\text{Ni}_{5.3}\text{P}_{22.8}$  were produced in an induction furnace by melting the raw elements (purity  $\geq 99.995\%$ ). The master

alloys were purified in the molten state under a flux of  $B_2O_3$  prior to casting. All samples were shown to be fully homogenous and x-ray amorphous prior to all experiments. The absolute specific heat capacity,  $C_p$ , of  $Pt_{60}Cu_{16}Co_2P_{22}$  was determined in this work with a Perkin Elmer Diamond DSC on heating in reference to the specific heat capacity of a standard sapphire using a step method described elsewhere [5]. The  $C_p$  data of the  $Pt_{57.3}Cu_{14.6}Ni_{5.3}P_{22.8}$  were published previously [6].

The determination of the equilibrium viscosity at temperatures close to the glass transition were carried out on both alloy compositions using the three-point beam-bending method of Ref. [7] in the a NETZSCH TMA 402 Thermo-Mechanical Analyzer as described in Ref. [8]. The fittings were performed with OriginPro 9.0, using a non-linear fitting procedure that applies the standard Chi-squared minimization test. For each viscosity dataset consistent VFT-fits and Adam-Gibbs fits are established by fitting to Eqs. (1) and (2), respectively, to the logarithmic values of viscosity plotted against inverse temperature.

The VFT-equation is:

$$\eta = \eta_0 \exp\left(\frac{D^*T_0}{T - T_0}\right), \quad (1)$$

where the fitting parameters are the kinetic fragility parameter,  $D^*$ , and the VFT-temperature,  $T_0$ . The Adam-Gibbs fits of the viscosity data were performed using Eq. (2), which is a relation between the viscosity and the configurational entropy of liquid,  $S_c(T)$ , as

$$\eta(\approx MD^{-1}) = \eta_0 \exp\left(\frac{C}{T \cdot S_c(T)}\right). \quad (2)$$

Here,  $D$  is the diffusivity,  $M$  is a multiplier that takes into account the Einstein relation between the diffusivity and mobility, and  $C$  is a constant that represents the free enthalpy barrier per particle to cooperative rearrangements.  $S_c(T)$  is the configurational part of the entropy, and represents the number of distinct packing states at a certain temperature. Through  $S_c$ , the fragility phenomenon is connected to

the topography of the potential energy surface. Since  $S_c(T)$  cannot be measured directly, in the present work it is assumed that the configurational entropy of the liquid decreases from the fixed value  $S_c(T_m^*)$  during undercooling with the same rate as the entropy difference between the liquid and the crystal, as

$$S_c(T) = S_c(T_m^*) - \int_T^{T_m^*} \frac{\Delta C_p^{l-x}(T')}{T'} dT'. \quad (3)$$

This is an assumption that is more appropriate than the direct use of the excess entropy change of the liquid to the crystal for expressing  $S_c(T)$ , and only  $C$  and  $S_c(T_m^*)$  are left as fitting parameters in Eq. (2). The value  $S_c(T_m^*)$  is a property exclusive to the liquid phase, defined for a fixed viscosity value of 1 Pa s, as established in Ref. [5]. The value of  $S_c(T_m^*)$  is independent of the entropy of the crystal state, and it is different from the entropy of fusion  $\Delta S^{l-x}(T_f)$ , which depends on the configurational entropy of the crystalline phase. Indeed, when applied to BMG systems, the Adam-Gibbs equation utilizing  $\Delta S^{l-x}(T) \approx S_c(T)$  has been shown to be a poor approximation [9-11]. The approximation made in Eq. (3) requires the assumption that the vibrational contribution to the total entropy of the supercooled liquid changes with undercooling approximately with the same rate as the vibrational contribution of the crystal's entropy. This is an assumption that has been shown to be more appropriate than the direct use of the excess entropy change of the liquid to the crystal for expressing  $S_c(T)$  [5, 11-12].

The calculation of the integral term in Eq. (3) requires fitting calorimetric specific heat capacity data of the liquid and of the crystal to the equations below:

$$C_p^l(T) = 3R + aT + bT^{-2};$$

$$C_p^s(T) = 3R/M \{1 - \exp[-1.5(T/T_D)]\} \quad (5), \text{ after ref. [13];}$$

$$C_p^x(T) = 3R + cT + dT^2 \quad (6), \text{ valid at temperatures far above the Debye temperature (TD);}$$

$$C_p^x(T) = 3R/M \{1 - \exp[-1.5(T/T_D)]\} \quad (7), \text{ valid at low temperatures [13];}$$

$$\Delta C_p^{l-x}(T) = C_p^l(T) - C_p^x(T). \quad (8)$$

The constants  $a$ ,  $b$ ,  $c$ , and  $d$  are fitting constants,  $R$  is the universal gas constant, and  $T$  is the absolute temperature. The low  $T_{liq}$  of these alloys permit us to measure the absolute specific heat capacity of the crystal and of the melt using solely DSC. By means of Eq. (3), the temperature at which the configurational entropy vanishes, i.e.  $S_c(T) = 0$  was calculated and denoted hereafter as  $T_0^*$ .

### 3. RESULTS AND DISCUSSION

The isothermal data of the specific heat capacity of amorphous, crystalline, and liquid  $\text{Pt}_{60}\text{Cu}_{16}\text{Co}_2\text{P}_2$  are shown in Fig. 1 as scatter symbols. The temperatures indicated in the plot are listed in Table Ia.  $T_g^*$  marks the glass transition temperature as calculated with Eq. (1) for a viscosity value of  $10^{12} \text{ Pa s}$ .  $T_{liq}$  marks the end temperature of the melting event (liquidus temperature) as detected in DSC (880 K).  $T_0^*$  indicates the temperature at which the configurational entropy of the liquid vanishes. This temperature is determined by setting Eq. (3) equal to zero. For this alloy the heat of fusion,  $\Delta H_f$ , measured in DSC, is 10.7 kJ (g-atom)<sup>-1</sup>. With this value, the entropy of fusion is calculated as  $\Delta S_f = 12.8 \text{ J(g-atom K)}^{-1}$ , a higher value with respect to those for the Zr-based BMG alloys of about  $8.5 \text{ J(g-atom K)}^{-1}$  [9,11] and twice as high as those of the Pd-Cu-Ni-P alloys [6]. The Kauzmann temperature is  $T_K = 412 \text{ K}$ , which is the temperature at which the total entropy of the supercooled liquid becomes equal to that of the crystalline mixture.

The fits of Eq. (4) to the experimental specific heat capacity data of the liquid and solid states for the  $\text{Pt}_{60}\text{Cu}_{16}\text{Co}_2\text{P}_2$  are shown in Fig. 1 as the dashed and solid curves, respectively. The parameters  $a$ ,  $b$ ,  $c$ , and  $d$  are  $5.46846 \times 10^{-3} \text{ J/g-at}\cdot\text{K}^2$ ,  $6.2676 \times 10^6 \text{ J}\cdot\text{K/g-at}$ ,  $-1.2242 \times 10^{-3} \text{ J/g-at}\cdot\text{K}^2$ , and  $7.7265 \times 10^{-6} \text{ J/g-at}\cdot\text{K}^3$ , respectively. The multiplier  $M$  is 0.97 and 0.96 for the

crystal and the glass, respectively. For the  $\text{Pt}_{57.3}\text{Cu}_{14.6}\text{Ni}_{5.3}\text{P}_{22.8}$ , the  $a$ ,  $b$ ,  $c$ ,  $d$  parameters were determined in Ref. [5].

The value of  $\Delta C_p^{L-X}(T)$ , scaled by the  $C_p(T)$  of the crystal for the studied BMG forming liquids are plotted in Fig. 2 against the  $T_m^*$ -scaled temperature in comparison to a stronger liquid of the Zr-Ti-Cu-Ni-Be system. The scaling-parameter  $T_m^*$ , is the temperature for which the viscosity of the melt is fixed at 1 Pa s and its values are listed in Table Ib. The example reported in Fig. 2 is for the stronger BMG former Vitreloy 1b, taken from Ref. [11], where  $T_m^*$  value of 1319 K. The increase in  $C_p$  at the glass transition (here indicated as  $T_g^*$ ) is generally larger for the fragile liquids and smaller for strong liquids [14-15]. The two Pt-based liquids studied here behave thermodynamically similar and in general much more fragile than the Zr-based liquids. Since a higher  $C_p$  indicates a faster change in enthalpy and entropy, it can be hypothesized that the structural changes of the Pt-alloys are more drastic above the melting point in comparison to the stronger Zr-based alloys.

Fig. 3 shows the equilibrium viscosity values (symbols) measured for the two studied Pt-based compositions from isothermal three-point beam-bending experiments in the vicinity of the glass transition. The values are plotted on a logarithmic scale against  $T_g^*$ -scaled inverse temperature and are determined at longer annealing times when the viscosity reaches a constant value after an initial relaxation. The equilibrium viscosities were obtained by fitting the relaxation curves with the Kohlrausch–Williams–Watts (KWW) stretched exponential function as described in Ref. [11]. The VFT-parameters,  $D^*$  and  $T_0$ , are listed in Table Ib. A VFT-fit of the relaxation times calculated from the DSC  $T_g$ -shift due to different heating rates lead previously to an apparent stronger behavior for the  $\text{Pt}_{57.3}\text{Cu}_{14.6}\text{Ni}_{5.3}\text{P}_{22.8}$ , ( $D^* \cong 16$  [5-6]). This apparent stronger behavior was proved recently [16] to reflect the cooling rate applied to the samples prior the DSC scans. Thus, the relaxation times taken from scans where the cooling rate is equal the heating rate would have been more appropriate in Ref. [5-6]. In this study, a fragility parameter of  $D^* = 11.8$  for  $\text{Pt}_{57.3}\text{Cu}_{14.6}\text{Ni}_{5.3}\text{P}_{22.8}$ , obtained by fitting the isothermal viscosity data is more representative for this system.

In comparison to Zr-based BMGs, the two Pt-based compositions studied here show a distinctively more fragile behavior. Fragility parameters with values as low as 12 have been measured in molten state by Busch and co-workers by rotating concentric-cup rheometry for various BMG forming liquids. For example, the  $\text{Zr}_{41.2}\text{Ti}_{13.8}\text{Cu}_{12.5}\text{Ni}_{10}\text{Be}_{22.5}$  behaves as a very fragile liquid at high temperatures ( $D^*=12$ ), then



undergoes a fragile-to-strong transition during undercooling. Its  $D^*$  parameter rises accordingly, to as high as 26.4 [17].

Additionally, nonlinear fits of the Adam-Gibbs equation [Eq. (2)] by means of Eq. (3) were applied to the experimental viscosity data. The Adam-Gibbs parameters are listed in Table Ib. The configurational entropy,  $S_c(T)$ , of each glass former is plotted normalized by  $S_c(T_m^*)$  in Fig. 4 as a function of  $T_m^*$ -scaled temperature. The apparent maximum for Vitreloy 1b is an artifact of the  $C_p$  measurements, i.e., extrapolation of the crystalline data to temperatures higher than the melting point leads to an apparent crossing of the  $C_p^l(T)$ , and  $C_p^x(T)$  curves. For better comparison the data corresponding the Vitreloy 4 ((from Ref [5]) are added to the plot. For each glass former the temperature at which the configurational entropy of the liquid vanishes, denoted as  $T_0^*$ , is represented by the intercepts with the x-axis in Fig. 4. The configurational entropy of the liquid vanishes at  $T_0^*$  and is in the range of  $(0.30-0.33)T_m^*$  for the stronger Zr-based BMG alloys, whereas for the more fragile systems based on Pt-P the  $S_c$  vanishes at higher temperatures, at  $T_0^* \cong 0.45-0.5 T_m^*$ . The latter value is comparable to the value of  $T_0^*$  found in Ref. [5] for most of the Pd-(Cu)-Ni-P glass forming liquids. The value of  $T_0$  obtained from the VFT fits matches the temperature ( $T_0^*$ ) where the configurational entropy vanishes in the Adam-Gibbs fits and suggests the same microscopic origin for thermodynamic and kinetic fragility. When the configurational entropy of the liquid vanishes only one distinct packing state is possible. This leads to the smallest possible potential energy of the system. The fact that the kinetic  $T_0$  and the thermodynamic  $T_0^*$  are similar indicates that when the barrier with respect to viscous flow becomes infinitely large (at  $T_0$ ), the liquid will act like a solid that has assumed the ideal packing configuration. According to Angell [18], liquids that structurally have a well-defined bonding scheme are restricted in placing particles in space and result in a low density of potential energy minima in comparison to liquids that lack such network bonding schemes. According to the Adam-Gibbs theory, a low density of potential minima would imply a less Arrhenius behavior (non-linear behavior) of the viscosity and therefore a VFT-type behavior typical of more fragile glasses. In BMG forming liquid systems, the icosahedral clusters (or icosahedral short-range order) found in Zr-based liquids restrict, from a kinetics point of view, the redistribution of the component elements across the icosahedral liquid [19], and places them among the strongest metallic glasses. The highly dense, randomly packed structure of these BMGs in their supercooled state results in extremely low atomic mobility [4,20], and yields small entropy of fusion values, due of the large amount of order in the liquid, with respect to liquids that would lack short-range order altogether. The present Pt-Cu-Ni-P and Pt-Cu-Co-P BMG alloys have very low kinetic fragility values, and therefore, can be considered among the most

fragile BMG glasses. They also have larger entropy of fusion values than Zr- based alloys, which indicates that their liquids have a limited amount of order (certainly less ordered than the icosahedral short-range order). This could even be more pronounced in the case of crystalline phases are at a very low entropic level, i.e. highly ordered. The Pt-based BMG forming liquids are expected to exhibit a strong bonding nature between the metal–metalloid atomic pairs; nevertheless, this seems not to affect their apparently fragile nature. In comparison, in the fragile Pd-based glass forming liquids, two large clustered units of a trigonal prism capped with three half-octahedra for Pd–Ni–P and a tetragonal dodecahedron for the Pd–Cu–P region were identified [21-22]. The coexistence of these two large different clustered units is considered an important role in the stabilization of the supercooled liquid for the Pd-based alloys [19], which is reflected in the low entropy of fusion values. In contrast to the Pd-based alloys, the Pt-based BMGs studied here exhibit among the highest values of entropy of fusion measured for BMG systems, and this could indicate that the microscopic origin of their fragile behavior follows a different scheme. Pronounced medium range order might not exist in the melt or it may be established at lower  $T$ , lower than  $T_g$ . It could also be possible that above the liquidus they exhibit even more fragile behavior ( $D^* < 10$ ). This can be tested, for example, by rheology experiments in the high-temperature melt.

The  $Sc(T_m^*)$  entropy parameter has high absolute values. This is observed in all multicomponent BMG systems [5,11-12], and implies the existence of a considerable amount

of excess configurational entropy, present in the melt at  $T_m^*$ , that in a multicomponent likely results from the entropy of mixing

In terms of the Adam–Gibbs theory, the free enthalpy barrier for cooperative rearrangements,  $C$ , is an important factor which is connected to the small displacement of atoms, while the cooperative group remains the same or at least has the same dependence on temperature as for structural relaxation [18]. The stronger the glass-forming liquid, the larger the  $C$ . In Ref. [5],  $C$  increases from about  $150 \text{ kJ (g-atom)}^{-1} \text{ K}^{-1}$  for the most fragile liquids (similarly to the studied Pt-based compositions) to about  $300 \text{ kJ (g-atom)}^{-1} \text{ K}^{-1}$  for the strongest Zr-based alloys (for example Vitreloy 1). These values compare well to the activation energies for diffusion in the glass around the glass transition temperature of about 1 eV for small atoms and 3 eV for large atoms [22]. In the light of the discussion about cooperativity and correlation lengths, if the present fragile Pt-based BMG forming liquids require a lower activation barrier, the atomic flow or the relaxation event is less localized and involve small atoms and therefore is, in a sense, more liquid-like than in the Zr-based liquids.

### 3. CONCLUSIONS

In summary, the isothermal viscosities of  $\text{Pt}_{60}\text{Cu}_{16}\text{Co}_2\text{P}_{22}$  and  $\text{Pt}_{57.3}\text{Cu}_{14.6}\text{Ni}_{5.3}\text{P}_{22.8}$  were determined during annealing at temperatures around  $T_g$  and the temperature dependence of the equilibrium viscosity was found to be well described by both the VFT equation and Adam-Gibbs configurational entropy model. The fragility parameter  $D^*$  is determined to be 10.8 and 11.8, respectively, and the C-parameter from the Adam-Gibbs equation was determined to be 146.75 and 158.56 kJ g-atom<sup>-1</sup>, respectively, values that are among the smallest determined for BMG forming liquids. In comparison with the Zr-based glasses, the Pt-Cu-(Ni,Co)-P glasses have a distinctly larger increase in the specific heat capacity at the glass transition and high entropy of fusion values, which is twice that of Pd-based alloys. These values reflect that the microscopic origin of their fragile behavior of the Pt-based alloys follow a different scheme than that identified for both the Zr- based alloys and the Pd-based alloys.

### Acknowledgements

This research was supported by the *Deutsche Forschungsgemeinschaft* (German Research Foundation) through Grant No. GA 1721/2-1. Additional support was provided by the German Federation of Industrial Research Associations (AiF/IGF) through Project No. 16843N. The authors wish to thank J. Schroers for useful discussions regarding the preparation of the alloys, L. Battezzati for useful discussion throughout the exchange of GdF and to express their gratitude to C. Hafner *Edemetall Technologie* for the platinum supply.

## REFERENCES

- [1] R. Busch, E. Bakke, and W.L. Johnson, Viscosity of the supercooled liquid and relaxation at the glass transition of the  $\text{Zr}_{46.75}\text{Ti}_{8.25}\text{Cu}_{7.5}\text{Ni}_{10}\text{Be}_{27.5}$  bulk metallic glass forming alloy *Acta Mater.* 46 (1998) 4725-4732.
- [2] J. Schroers, Y. Wu, and R. Busch, W.L. Johnson, Transition from nucleation controlled to growth controlled crystallization in  $\text{Pd}_{43}\text{Ni}_{10}\text{Cu}_{27}\text{P}_{20}$  melts, *Acta Mater.* 49 (2001) 2773-2781.
- [3] L. Shownspeaker and R. Busch, On the fragility of Nb-Ni-based and Zr-based bulk metallic glasses, *Appl. Phys. Lett.* 85 (2004) 2508-2510.
- [4] R. Busch, J. Schroers, W.H. Wang, Thermodynamics and kinetics of bulk metallic glass, *MRS Bull.* 32 (2007) 620-623.
- [5] I. Gallino, J. Schroers, R. Busch, Kinetic and thermodynamic studies of the fragility of bulk metallic glass forming liquids, *J. Appl. Phys.* 108 (2010) 063501.
- [6] B.A. Legg, J. Schroers, R. Busch, Thermodynamics, kinetics, and crystallization of  $\text{Pt}_{57.3}\text{Cu}_{14.6}\text{Ni}_{5.3}\text{P}_{22.8}$  bulk metallic glass, *Acta Mater.* 55 (2007) 1109-1116.
- [7] H.E. Hagy, Experimental Evaluation of Beam-Bending Method of Determining Glass Viscosities in the Range 108 to 1015 Poises, *J. Am. Ceram. Soc.* 46 (1963) 93-97.
- [8] Z. Evenson, S. Raedersdorf, I. Gallino, R. Busch, Equilibrium viscosity of Zr-Cu-Ni-Al-Nb bulk metallic glasses, *Scripta Mater.* 63 (2010) 573-576.
- [9] I. Gallino, M.B. Shah, R. Busch, Enthalpy relaxation and its relation to the thermodynamics and crystallization of the  $\text{Zr}_{58.5}\text{Cu}_{15.6}\text{Ni}_{12.8}\text{Al}_{10.3}\text{Nb}_{2.8}$  bulk metallic glass forming alloy, *Acta Mater.* 55 (2007) 1367-1376.
- [10] G. Fiore, L. Battezzati, Thermodynamic properties of the  $\text{Pd}_{77.5}\text{Cu}_6\text{Si}_{16.5}$  undercooled liquid, *J. of Alloys and Compounds* 483 (2009) 54-56.
- [11] Z. Evenson, R. Busch, Equilibrium viscosity, enthalpy recovery and free volume relaxation in a  $\text{Zr}_{44}\text{Ti}_{11}\text{Ni}_{10}\text{Cu}_{10}\text{Be}_{25}$  bulk metallic glass, *Acta Mater.* 59 (2011) 4404-4415.

- [12] R. Busch, W. Liu, W.L. Johnson, Thermodynamics and kinetics of the Mg<sub>65</sub>Cu<sub>25</sub>Y<sub>10</sub> bulk metallic glass forming liquid, *J. Appl. Phys.* 83(8) (1998) 4134-4141.
- [13] S. Inaba, S. Oda, K. Morinaga, Heat Capacity of oxide glasses at high temperature region, *J. of Non-crystall. Solids* 325 (2003) 258-266.
- [14] C.A. Angell, Formation of glasses from liquids and biopolymers, *Science* 267 (1995) 1924-1935.
- [15] G. Dalla Fontana, L. Battezzati, Thermodynamic and dynamic fragility in metallic glassformers, *Acta Mater.* 61 (2013) 2260-2267.
- [16] Z. Evenson, I. Gallino, R. Busch, The effect of cooling rates on the apparent fragility of Zr-based bulk metallic glasses, *J. Appl. Phys.* 107 (2010) 123529.
- [17] C. Way, P. Wadhwa, R. Busch, The influence of shear rate and temperature on the viscosity and fragility of the Zr<sub>41.2</sub>Ti<sub>13.8</sub>Cu<sub>12.5</sub>Ni<sub>10.0</sub>Be<sub>22.5</sub> metallic-glass-forming liquid *Acta Mater.* 55 (2007) 2977-2983.
- [18] C.A. Angell, Relaxation in liquids, polymers and plastic crystals - strong/fragile patterns and problems, *J. Non-Cryst. Solids* 131–133 (1991) 13-31.
- [19] W.H. Wang, C. Dong, C.H. Shek, Bulk metallic glasses, *Mater. Sci. Engi. R* 44 (2004) 45–89.
- [20] A. Inoue, T. Negishi, H.M. Kimura, T. Zhang, A.R. Yavari, High packing density of Zr and Pd-based bulk amorphous alloys, *Mater. Trans. JIM* 39 (1998) 318-321.
- [21] A. Inoue, A. Takeuchi, Recent progress in bulk glassy alloys, *Mater. Trans. JIM* 43 (2002) 1892-1906. 11
- [22] F. Faupel, W. Frank, M.P. Macht, H. Mehrer, V. Naundorf, K. Ratzke, H.R. Schober, S.H. Sharma, and H. Teichler, Diffusion in metallic glasses and supercooled melts, *Rev. Mod. Phys.* 75 (2003) 273-280.

TABLE CAPTION

Table I: Thermodynamic and kinetic parameters for the glass formers of this study in the same order as they are obtained during the fitting procedures.

(a)  $T_g$  and  $T_x$  are the onsets of the glass transition and the crystallization measured in DSC at  $0.33\text{ K s}^{-1}$ ;  $T_{eut}$  is the eutectic temperature,  $T_f$  is the peak temperature of fusion;  $T_{liq}$  is the liquidus temperature;  $a, b, c, d$  the specific heat capacity parameters of Eqs. (5);  $\Delta H_f$  is the enthalpy of fusion measured in DSC;  $\Delta S_f$  is calculated as  $\Delta H_f/T_f$ ;  $T_K$  is the calculated Kauzmann temperature.  
(b)  $D^*$  and  $T_0$  are the VFT parameters of Eq. (1);  $T_g^*$  and  $T_m^*$  are the temperatures at which the glass former and the melt assume values of  $10^{12}\text{ Pa s}$  and  $1\text{ Pa s}$ , respectively.  $T_0^*$  is the temperature at which the configurational entropy of the glass former is zero.  $S_c(T_m^*)$  is the configurational entropy of the liquid at  $T_m^*$ ;  $C$  is the free enthalpy barrier per particle to cooperative rearrangements.

Table I.

(a) Thermodynamic parameters measured using DSC

	$T_g$	$T_x$	$T_{eut}$	$T_f$	$T_{liq}$	$\Delta H_x$	$\Delta H_f$	$\Delta S_f$	$T_K$
	K	K	K	K	K	kJ/g-at	kJ/g-at	J/g-at·K	K
Pt <sub>60</sub> Cu <sub>16</sub> Co <sub>2</sub> P <sub>22</sub>	506	573	824	835	880	8.4	10.7	12.8	412
Pt <sub>57.3</sub> Cu <sub>14.6</sub> Ni <sub>5.3</sub> P <sub>22.8</sub> <sup>a</sup>	501	577	735	754	833	7.7	11.4	14.7	396

<sup>a</sup> from ref. [6]

(b) VFT and Adam-Gibbs parameters

Material	$D^*$	$T_0$	$T_0^*$	$T_m^*$	$S_c(T_m^*)$	$C$	$T_g^*$
		K	K	K	J/g-at·K	kJ/g-at	K
Pt <sub>60</sub> Cu <sub>16</sub> Co <sub>2</sub> P <sub>22</sub>	10.8	375	375	774	17.74	146.75	482
Pt <sub>57.3</sub> Cu <sub>14.6</sub> Ni <sub>5.3</sub> P <sub>22.8</sub>	11.8	362	375	784	18.20	158.57	475

FIGURE CAPTIONS

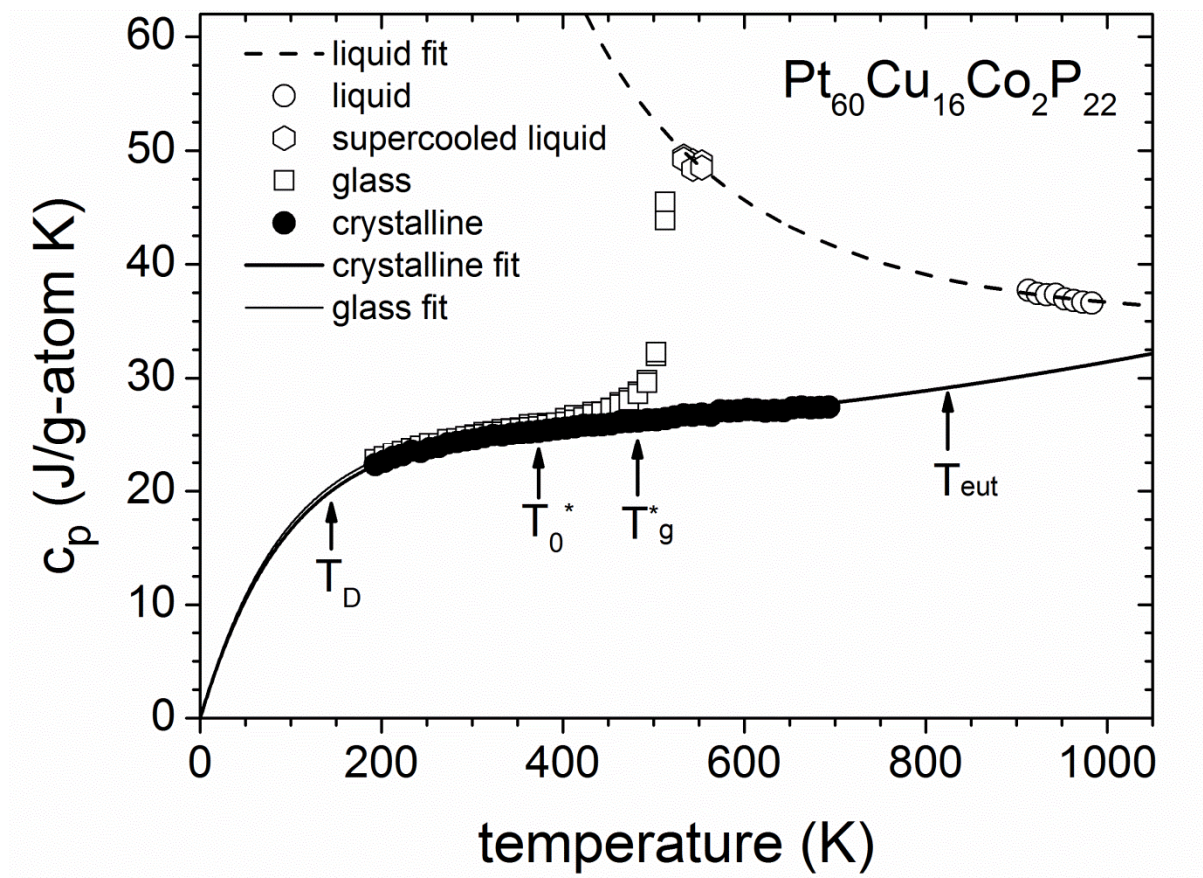


Figure 1: Isothermal specific heat capacity data for  $\text{Pt}_{60}\text{Cu}_{16}\text{Co}_2\text{P}_{22}$  as a function of

temperature. The symbols are data for the glass (open square), the crystalline solid (closed circles), the supercooled liquid (open hexagons), and the liquid state (open circles). The data were measured in steps in reference to sapphire from 193 K. The error bar has the size of the symbols. The curves represent the fits to Eqs. (4-7).  $T_g^*$  and  $T_{\text{eut}}$  mark the glass transition temperature at which the supercooled liquid assumes a value of  $10^{12}$

Pa s (482 K), and the calorimetric eutectic temperature (824 K), respectively.  $T_0^*$  marks the temperature at which the configurational entropy of the liquid vanishes (376 K).  $T_D$  is the Debye temperature (144.5 K for the glass and 139.8 K for the crystal).

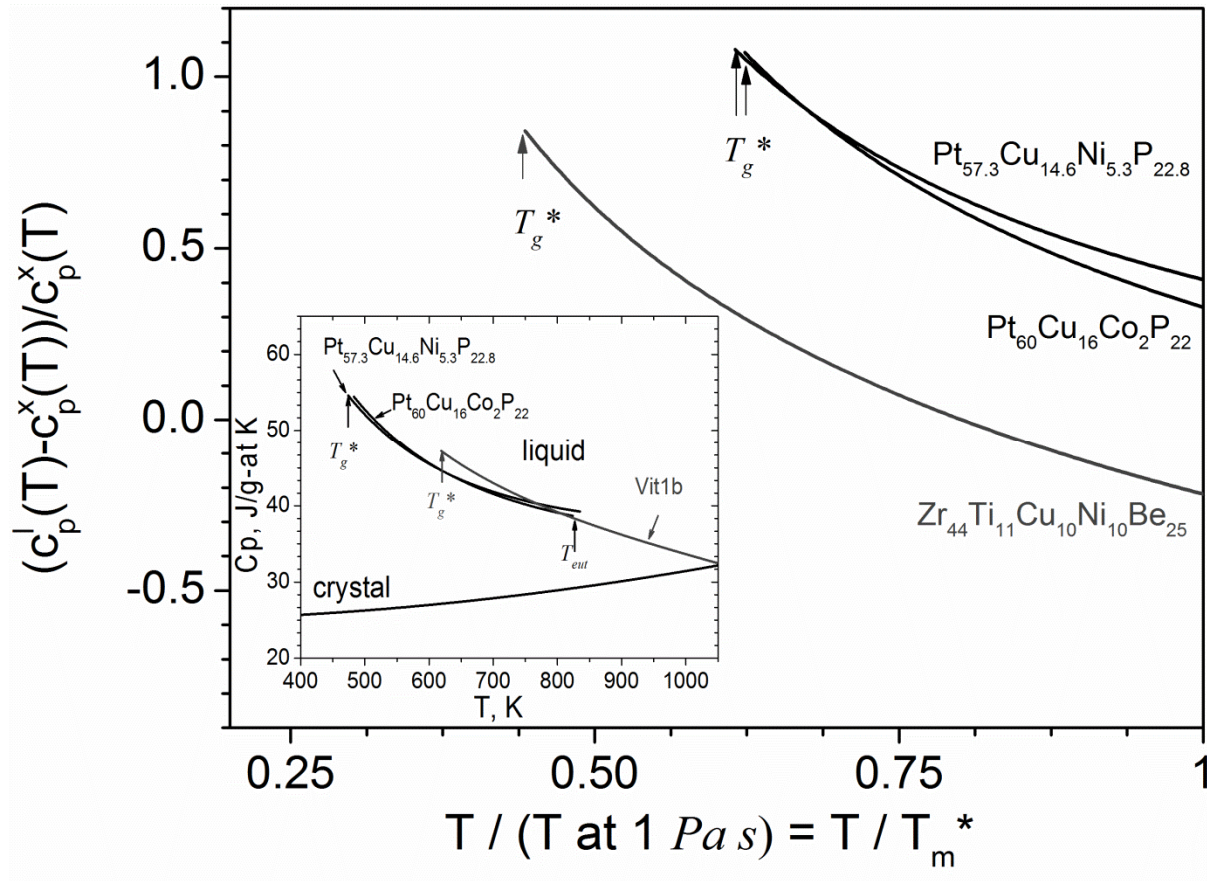


Figure 2: Specific heat capacity differences between the liquid and the crystal, normalized by the  $C_p$  of the crystal, as a function of temperature normalized by  $T_m^*$ , the temperature at which the viscosity of the liquid assumes a value of 1 Pa s. The curves are calculated from Eqs. (4) using the parameters obtained from this study for  $\text{Pt}_{60}\text{Cu}_{16}\text{Co}_2\text{P}_{22}$ , from Ref. [5] for the  $\text{Pt}_{57.3}\text{Cu}_{14.6}\text{Ni}_{5.3}\text{P}_{22.8}$ , and from [11] for the  $\text{Zr}_{44}\text{Ti}_{11}\text{Ni}_{10}\text{Cu}_{10}\text{Be}_{25}$ . In the inset, the specific heat

capacities in the supercooled liquid are plotted with respect to the  $C_p(T)$  function of the  $\text{Pt}_{60}\text{Cu}_{16}\text{Co}_2\text{P}_{22}$  crystalline state against absolute temperature.



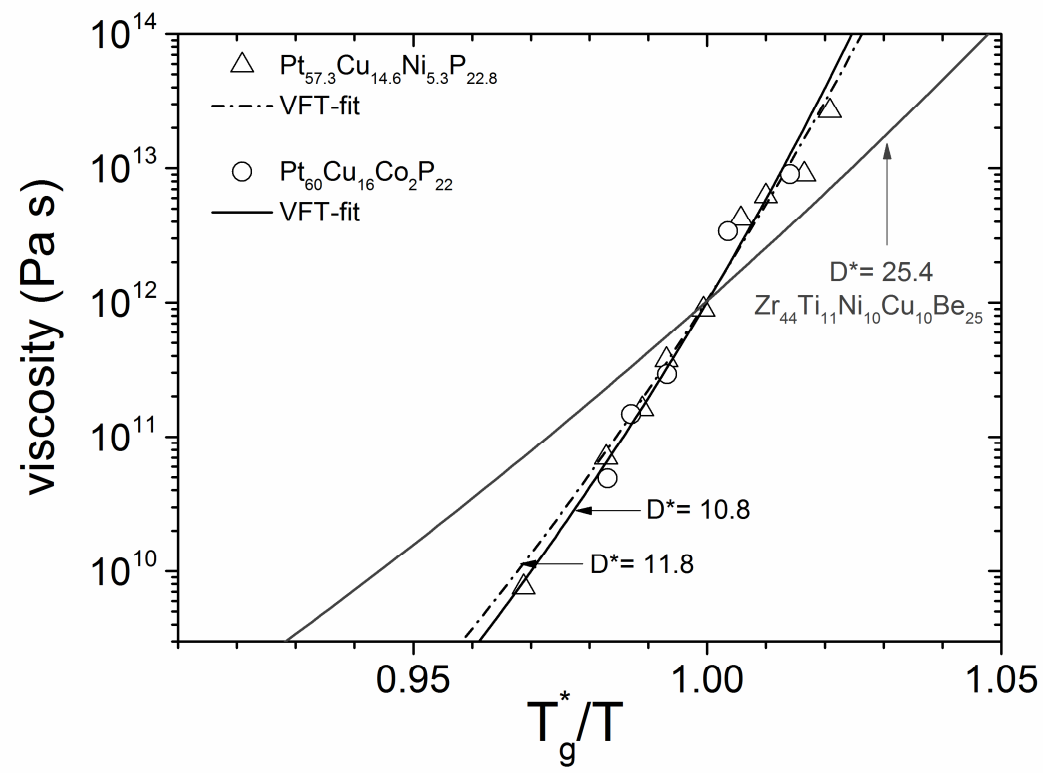


Figure 3: Equilibrium viscosity values (symbols) measured from isothermal three-point beam-bending experiments in the vicinity of the glass transition for  $\text{Pt}_{60}\text{Cu}_{16}\text{Co}_2\text{P}_{22}$  and  $\text{Pt}_{57.3}\text{Cu}_{14.6}\text{Ni}_{5.3}\text{P}_{22.8}$  as determined in this study. The scaling temperature  $T_g^*$  is the temperature at which the supercooled liquid assumes a value of  $10^{12}$  Pa s. The continuous lines are the fits to the VFT- equation [Eq. (1)]. The VFT fit for  $\text{Zr}_{44}\text{Ti}_{11}\text{Ni}_{10}\text{Cu}_{10}\text{Be}_{25}$  made use of the parameters from Ref. [11].

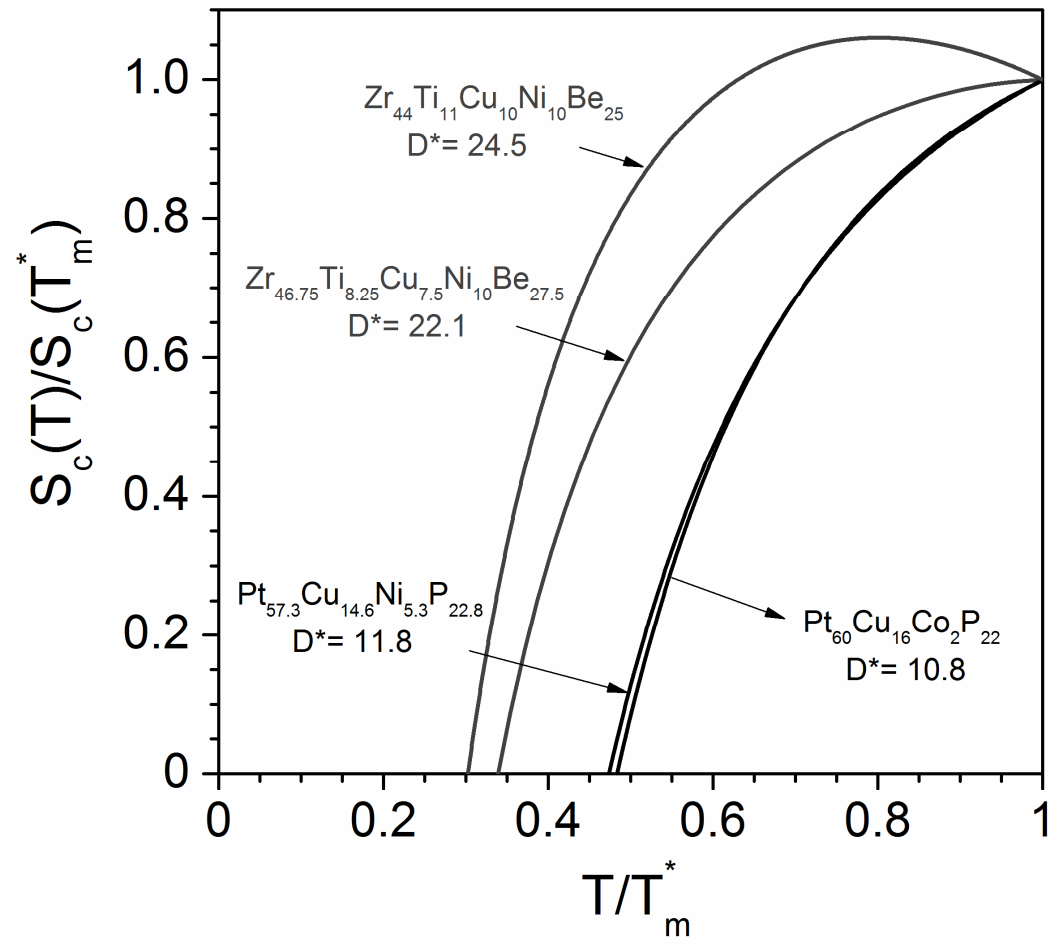


Figure 4: Normalized configurational entropy plot of the  $\text{Pt}_{60}\text{Cu}_{16}\text{Co}_2\text{P}_{22}$ ,  $\text{Pt}_{57.3}\text{Cu}_{14.6}\text{Ni}_{5.3}\text{P}_{22.8}$  and  $\text{Zr}_{44}\text{Ti}_{11}\text{Ni}_{10}\text{Cu}_{10}\text{Be}_{25}$  (Vitrelloy 1b) and  $\text{Zr}_{46.75}\text{Ti}_{8.25}\text{Ni}_{10}\text{Cu}_{7.5}\text{Be}_{27.5}$  Vitrelloy 4 (using parameters from Ref. [11] and [5], respectively) BMG forming liquids as a function of temperature. The normalization is against the configurational entropy of the liquid for a temperature,  $T_m^*$ , at which the viscosity is of 1 Pa s. The temperature at which the configurational entropy of the liquid,  $S_c$ , vanishes is  $T_0^*$ , which is about  $T_m^*/3$  for Zr-based BMGs, and is about  $T_m^*/2$  for the Pt-based BMGs.